Progress in Oceanography 79 (2008) 366–378

Contents lists available at ScienceDirect

Progress in Oceanography

journal homepage: www.elsevier.com/locate/pocean

Trophic modeling of the Northern Humboldt Current Ecosystem, Part II: Elucidating ecosystem dynamics from 1995 to 2004 with a focus on the impact of ENSO

Marc H. Taylor [a,*], Jorge Tam [b], Verónica Blaskovic [b], Pepe Espinoza [b], R. Michael Ballón [b,c], Claudia Wosnitza-Mendo [b], Juan Argüelles [b], Erich Díaz [b], Sara Purca [b], Noemi Ochoa [d], Patricia Ayón [b], Elisa Goya [b], Dimitri Gutiérrez [b], Luis Quipuzcoa [b], Matthias Wolff [a]

[a] Center for Tropical Marine Ecology, Fahrenheitstr. 6, 28359 Bremen, Germany
[b] Instituto del Mar del Perú, Esq. Gamarra y Valle s/n, Apartado 22, Callao, Peru
[c] IRD, UR097, CRH, Avenue Jean Monnet, 34203 Sete, France
[d] Universidad Nacional Mayor de San Marcos, Apartado 12, Lima, Peru

ARTICLE INFO

Article history:
Accepted 14 October 2008
Available online 21 October 2008

Keywords:
Coastal upwelling
Ecosystem disturbance
El Niño phenomena
Trophic relationships
Trophodynamic model
Peru Humboldt Current

ABSTRACT

The Northern Humboldt Current Ecosystem is one of the most productive in the world in terms of fish production. Its location near to the equator permits strong upwelling under relatively low winds, thus creating optimal conditions for the development of plankton communities. These communities ultimately support abundant populations of grazing fish such as the Peruvian anchoveta, *Engraulis ringens*. The ecosystem is also subject to strong inter-annual environmental variability associated with the El Niño Southern Oscillation (ENSO), which has major effects on nutrient structure, primary production, and higher trophic levels. Here our objective is to model the contributions of several external drivers (i.e. reconstructed phytoplankton changes, fish immigration, and fishing rate) and internal control mechanisms (i.e. predator-prey) to ecosystem dynamics over an ENSO cycle. Steady-state models and time-series data from the Instituto del Mar del Perú (IMARPE) from 1995 to 2004 provide the base data for simulations conducted with the program Ecopath with Ecosim. In simulations all three external drivers contribute to ecosystem dynamics. Changes in phytoplankton quantity and composition (i.e. contribution of diatoms and dino- and silicoflagellates), as affected by upwelling intensity, were important in dynamics of the El Niño of 1997–98 and the subsequent 3 years. The expansion and immigration of mesopelagic fish populations during El Niño was important for dynamics in following years. Fishing rate changes were the most important of the three external drivers tested, helping to explain observed dynamics throughout the modeled period, and particularly during the post-El Niño period. Internal control settings show a mix of predator–prey control settings; however a "wasp-waist" control of the ecosystem by small pelagic fish is not supported.

1. Introduction

Eastern Boundary Current Systems (EBCSs), including the Humboldt, Canary, Benguela, and California Currents, and in particular their nearshore upwelling zones, are among the most productive fishing areas in the world. High primary and secondary productivity support large biomasses of small planktivorous pelagic fish, or "small pelagics", which through predator/prey interactions can influence both higher and lower trophic levels (i.e. "wasp-waist" ecosystem control, Cury et al., 2000).

The Humboldt Current, and specifically, the Peruvian upwelling system, produces more fish landings than the other EBCSs (both total and on a per area basis). However, remote sensing-based estimates of primary production rank the Peruvian upwelling system only third, behind the Benguela and Canary Current systems (Carr, 2002). In a way, this apparent paradox supports early fishery hypotheses that emphasize quantity and quality of upwelling. The Peruvian upwelling system's proximity to the equator and large Rossby radius results in strong and sustained upwelling under relatively mild wind forcing (Cury and Roy, 1989; Bakun, 1996). These conditions create a "particularly rich, non-turbulent, benign environment" by which rich coastal plankton communities develop and persist, in turn supporting abundant populations of small pelagics (Bakun and Weeks, 2008).

Peru's proximity to the equator also means that Kelvin waves traveling eastward along the equator during El Niño (EN) impact Peru almost directly. During EN, the "basin-wide ecosystem" of

* Corresponding author. Tel.: +49 4212380056; fax: +49 4212380030.
E-mail address: marchtaylor@yahoo.com (M.H. Taylor).

0079-6611/$ - see front matter © 2008 Elsevier Ltd. All rights reserved.
doi:10.1016/j.pocean.2008.10.008

the Pacific, which normally maintains a slope in sea level, thermal structure, and nutrient structure due to trade winds, is lost or reversed (Chavez et al., 2003; Pennington et al., 2006). While upwelling-favorable wind may continue along the Peruvian coast, water is upwelled from above the now deep thermocline and nutricline. As a result, primary production of the Peruvian upwelling system is reduced, and the "active zone" of high primary production can be 1/10th the size of normal conditions (Nixon and Thomas, 2001).

Under normal conditions diatoms dominate the nearshore phytoplankton community. Diatoms are particularly adapted to upwelling conditions through high doubling rates and their ability to form resting spores, which sink and are subsequently returned to the surface via upwelling (Pitcher et al., 1992). In the Humboldt Current system, EN reduces the upwelling of nutrient-rich water, which results in a reduction of the larger size fraction of the phytoplankton community (e.g. diatoms) (Bidigare and Ondrusek, 1996; Landry et al., 1996; González et al., 1998; Iriarte and González, 2004) and are replaced by subtropical phytoplankton normally found further offshore in nutrient poor waters (Rojas de Mendiola, 1981; Ochoa et al., 1985; Avaria and Muñoz, 1987). These changes in the phytoplankton produce changes throughout the ecosystem, with energy likely passing through different pathways before reaching a particle size suitable for grazing by small pelagics (Sommer et al., 2002; González et al., 2004; Iriarte and González, 2004; Tam et al., 2008).

This straightforward, bottom-up perspective becomes complicated when one considers the effects and interactions of top-down processes such as predation and fishing. Fortunately, trophic modeling of EBCSs has a long history from which to draw upon; including steady-state models of the Peruvian (Walsh, 1981; Baird et al., 1991; Jarre et al., 1991; Jarre-Teichmann, 1992) and other upwelling systems (Shannon et al., 2003; Heymans et al., 2004; Neira and Arancibia, 2004; Neira et al., 2004; Moloney et al., 2005). The development of the program Ecopath with Ecosim (EwE) (Walters et al., 1997) further allows for temporal explorations of dynamics, and has been previously applied to the southern Benguela system (Shannon et al., 2004a,b). A review of these advances (Taylor and Wolff, 2007) has assisted in the construction of new steady-state models for the Peruvian system as presented by Tam et al. (2008), which form the basis for the dynamic simulations presented here.

Our objectives are to elucidate the mechanisms of ecosystem dynamics in the Peruvian upwelling system over an ENSO cycle. We evaluate the importance of three external drivers: (i) changes in phytoplankton biomass and composition, (ii) immigration of mesopelagic fish into the model area, and (iii) changes in fishing rates. We also explore internal predator-prey control settings between functional groups of organisms (e.g. bottom-up, top-down control). We speculate that the degree of upwelling and resulting primary productivity may similarly affect ecosystem dynamics across seasonal, inter-annual (EN), and multi-decadal temporal scales, but use the data-rich period of 1995–2004 as a starting point for model exploration.

2. Methods

Using the temporal dynamic routine of Ecosim within the EwE package (Walters et al., 1997, 2000) we explored the relative importance of external and internal ecosystem drivers in the Northern Humboldt Current Ecosystem from 1995 to 2004. External, non-trophically-mediated drivers considered were changes in phytoplankton biomass, fishing rate (effort and mortality), and oceanic immigrant biomass (mesopelagic fish). Internal, trophically-mediated, factors concerned an exploration of trophic flow controls (e.g. bottom-up, top-down) that govern predator-prey dynamics.

2.1. Description of the model

The steady-state model from Tam et al. (2008) is used here as input describing the initial ecosystem state (1995/96 model), which encompasses a full "biological year" (i.e. starting from about the middle of a calendar year). The spatial domain is from 4°S to 16°S and 60 nm offshore (ca. 111 km; see Fig. 1 in Tam et al., 2008). The models consisted of 33 functional groups including detritus, macrobenthos, 2 phytoplankton groups, 4 zooplankton groups, 8 pelagic fish groups, 2 cephalopod groups, 12 demersal fish groups (including 3 life-history stages for Peruvian hake, *Merluccius gayi peruanus*), seabirds, pinnipeds, and cetaceans. Groups were chosen based on similar trophic connections (both to predator and prey groups), similar production and consumption rates, and importance to fishery resources.

The simulations calculate biomass changes through time by solving the set of differential equations:

$$dB_i/dt = g_i\left[\sum_k Q_{ki}(t)\right] - \sum_j Q_{ij}(t) - MO_iB_i - \sum F_{if}(t)B_i \qquad (1)$$

for functional groups $i = 1,\ldots,n$. The first sum represents the food-consumption rate, Q, summed over prey types k of species i, and g_i represents the growth efficiency (proportion of food intake converted into production). The second sum represents the predation loss rates due to predators j of i. All Q's in these sums are calculated by Eq. (2), below. MO_i represents the instantaneous natural mortal-

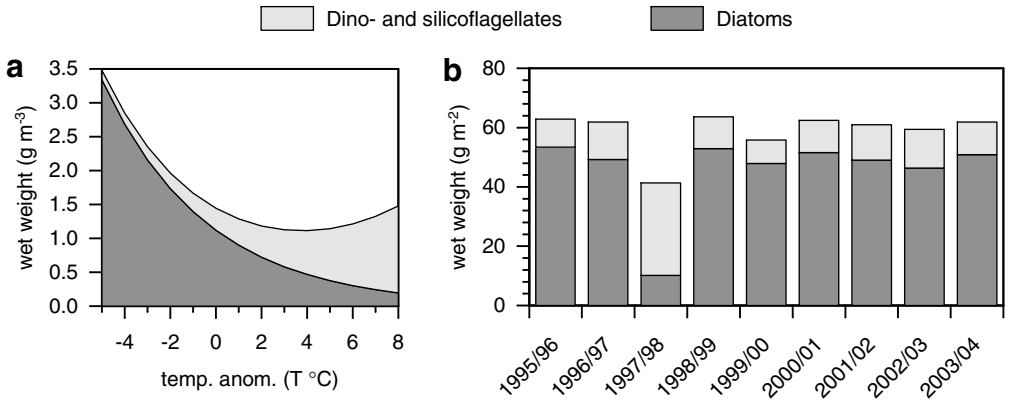

Fig. 1. (a) Relationship between coastal surface phytoplankton biomass (g m^{-3}) as a function of sea surface temperature anomaly (°C) and (b) reconstructed annual phytoplankton biomass values (g m^{-2}) used in the phytoplankton (*PP*) driver.

ity rate due to outside factors other than modeled predation. The final sum represents the instantaneous fishing mortality rate, F, as a sum of fishing components caused by fishing fleets f.

Consumption rates (Q_{ij}) are calculated by assuming that the biomass of prey i, B_i, is divided into vulnerable and safe components, and the flux rates v_{ij} and v'_{ij} move biomass into the vulnerable and safe pools, respectively. This assumption leads to the rate equation:

$$Q_{ij}\frac{a_{ij}(t)v_{ij}(t)B_iB_j}{v_{ij}(t)+v'_{ij}+a_{ij}(t)B_j} \quad (2)$$

where the total consumption rate Q_{ij} varies as a mass action product (avB_iB_j), and is modified downward by a "ratio dependent" effect ($v + v' + aB_j$) representing localized competition among predators. a_{ij} represents the rate of effective search by predator j for prey type i (for further information, see Walters and Martell, 2004). The vulnerabilities for each predator–prey interaction can be manipulated and settings will determine if control is top-down (i.e. Lotka-Volterra; $v > 2.0$), bottom-up (i.e., donor-driven; $v < 2.0$), or intermediate ($v \approx 2.0$). The EwE software can also fit the vulnerabilities ("fit-to-time-series" routine), where the sum of squares (SS) is minimized between observed and predicted log biomasses/catches:

$$SS = \sum [Log(B_{obs}) - Log(B_{pred.})]^2 \quad (3)$$

Simulations measured the importance of three external drivers (see Section 2.2) on dynamics of the Northern Humboldt Current Ecosystem from 1995 to 2004. In addition, we applied the "fit-to-time-series" search routine within EwE to determine a best possible combination of specific predator–prey controls (see Section 2.3). The simulation's performance was measured by SS against available time-series data of yearly biomass and catch changes. Time-series data were derived from biomass, catch, fisheries mortality, and fishing effort estimates from IMARPE (Instituto del Mar del Perú) and other sources (Table 1). These data were adapted to the model area and biological year averages.

2.2. External drivers

External drivers were not accounted for within the internal flows of the trophic model. These drivers included: (i) "*PP*", phytoplankton biomass changes due to changes in upwelling and nutrients; (ii) "*F*", fishing rate changes; and (iii) "*I*", Immigrant biomass changes, specifically, the expansion and immigration of mesopelagic fish into the model area. Drivers were introduced successively in all sequences and combinations in order to arrive to an average value of change in SS ($n = 15$). External driverś dynamics were defined by available or reconstructed long-term data series as described below.

Phytoplankton, *PP* – Long-term estimates of total phytoplankton biomass are available as total surface chlorophyll a (mg m^{-3}) from the SeaWifs satellite. We however needed to divide this total into the small- and large-sized phytoplankton functional groups, and did so by predicting functional group biomass from temperature anomaly, as below. We used a 1992–2000 time-series of coastal phytoplankton sampled by the Universidad Nacional Mayor de San Marcos (Lima, Peru) in Bahía de Ancón (77 39′ W–11 12′ S), Central Peru. The series consisted of cell counts of surface phytoplankton species, which were then converted to biovolume using cell dimensions gathered from literature sources or measured by microscopy. Cell dimensions were applied to geometric-shape assignments as described by Sun and Liu (2003) for the calculation of biovolume. Monthly average biovolume by taxonomic group were plotted against temperature anomalies off Ancón. Biovolume was natural log transformed and yielded the following linear relationships:

$$LN(B) = 17.841 - 0.2184 * T_{anom.} \quad (\text{Diatoms}, r = -0.20,\ p = 0.05) \quad (4)$$

$$LN(B) = 16.603 + 0.1719 * T_{anom.} \quad (\text{Dino- and silicoflagellates}, r = 0.14,\ p = 0.18) \quad (5)$$

where B = biovolume (μm^3 50 ml^{-1}), $T_{anom.}$ = temperature anomaly (°C). Typical of phytoplankton populations, a wide distribution of values was observed; however, diatom biovolume showed a negative trend and dino- and silicoflagellates a positive one, which is consistent with literature concerning the effects of ENSO on phytoplankton communities (Fig. 1a). These relationships were then applied to an index of integrated temperature anomalies for the entire Peruvian coast – the Peruvian Oscillation Index (POI) (Purca, 2005), which allowed for the reconstruction of coastal phytoplankton biovolumes for the years 1995–2003. Despite a non-significant correlation for dino- and silicoflagellates, the temperature-based predictions produce an acceptable range of surface phytoplankton biovolume when compared to the SeaWIFs data. For the simulations we use converted the temperature-based proportions of the two phytoplankton fractions to absolute values with the SeaWifs data for the model domain. Conversion factors used for chlorophyll a (Chl a) to wet weight were as follows: Chl a:Carbon (40:1) (Brush et al., 2002), and Carbon:wet weight (14.25:1) (Brown et al., 1991). Finally, a uniform mixed layer depth of 40 m was assumed to arrive at units of biomass per m^2 as described by Tam et al. (2008) (Fig. 1b).

Fishing rate, *F* – Time-series fishing rate estimates were only available for anchovy, hake and jumbo squid; however, these species represent key fisheries as well as important functional groups in the nearshore pelagic, nearshore demersal, and offshore pelagic ecosystems, respectively. These include fishing mortality rates derived from single species Virtual Population Analyses for anchovy and the three hake functional groups, and changes in fishing effort for jumbo squid (Table 2).

Immigration, I – While biomasses of several oceanic-associated functional groups apparently increased during EN (Tam et al., 2008), long-term data is only available for the mesopelagics functional group – lightfish and lanternfish – as determined by IMARPE acoustic surveys. Distribution of mesopelagics extends far offshore and thus we only considered the portion of the group in the model area. Mesopelagic's biomass increased in the model area following EN, apparently due to immigration; these changes were simulated by forcing mesopelagic biomass as an external driver.

2.3. Internal control

Model settings of prey vulnerability determine whether top-down bottom-up ecosystem dynamics dominate. "Mixed" or intermediate (*MX*; default $v = 2.0$) settings were used for initial explorations of the influence of external drivers. Afterwards, a further fit-to-time-series search routine was run for the 30 most sensitive predator–prey interactions (as determined by a sensitivity routine of the program) to reduce SS. The following interactions were also included to assess whether "wasp-waist" ecosystem control occurs around sardine and anchovy: (i) meso- and macrozooplankton as prey of sardine and anchovy; and (ii) all interactions where anchovy and sardine are prey. In total, 49 interactions were included in the search routine.

2.4. Focus on changes in main fishing targets

The dynamics of several main fishing targets and their interactions were also highlighted. Simulated mortality and diet changes for anchovy were examined in detail to help interpret

Table 1
Annual time-series data sets used in the Ecosim simulations.

Functional group	Data set	Comments	Used to force dynamics	Used to measure fit of simulation
1. Diatoms	Biomass (B)	SeaWifs; phytoplankton proportions reconstructed (see Section 2.3)	+	+
2. Dino- and silicoflagellates	Biomass (B)	SeaWifs; phytoplankton proportions reconstructed (see Section 2.3)	+	+
4. Mesozooplankton 200–2000 μm esd.	Biomass (B)	IMARPE survey (Ayón, personal communication) – corrected using seasonal anomalies (1959–2001)		+
7. Macrobenthos	Biomass (B)	IMARPE benthic survey (1995–2003) (Gutierrez and Quipuzcoa, personal communication)		+
8. Sardine – Sardinops sagax	Biomass (B)	IMARPE acoustic survey (1995–1999) (Gutierrez, personal communication)		+
	Catches (C)	Sea Around Us database (2006) (1995–2002)		+
9. Anchovy – *Engraulis ringens*	Biomass (B)	VPA estimates (1995–2003) (Niquen, personal communication)		+
	Fishing mortality (F)	VPA estimates (1995–2003)	+	
	Catches (C)	IMARPE catch statistics (1995–2003)		+
10. Mesopelagics – Lightfish and Lanternfish	Biomass (B)	IMARPE acoustic survey (1999–2003) (Gutierrez, personal communication)	+	+
11. Jumbo squid – Dosidicus gigas	Biomass (B)	IMARPE acoustic survey (1999–2003) (Arguelles, pers. comm.); 1995–1998 reconstructed from CPUE:acoustic ratio from 1999 to 2003		+
	Fishing effort (E)	Korean and Japanese industrial fleet data (1995–2003)	+	
	Catches (C)	Korean and Japanese industrial fleet data (1995–2003)		+
12. Other Cephalopods	Catches (C)	IMARPE catch statistics (1995–1999)		+
13. Other small pelagics – e.g. juvenile demersal fish	Catches (C)	Sea Around Us database (2006) – Engraulidae, Ethmidium maculatum (1995–2002)		+
14. Horse mackerel – Trachurus murphyi	Biomass (B)	IMARPE acoustic survey (1995–2003) (Gutierrez, personal communication)		+
15. Characteristic large pelagic – Scomber japonicus	Biomass (B)	IMARPE acoustic survey (1995–2003) (Gutierrez, personal communication)		+
16. Other large pelagics	Catches (C)	IMARPE catch statistics (1995–1999)		+
17. Small hake – Merluccius gayi peruanus (<29 cm)	Biomass (B)	VPA estimates (1995–2003) (Wosnitza-Mendo, personal communication)		+
	Fishing mortality (F)	VPA estimates (1995–2003)	+	
	Catches (C)	IMARPE catch statistics (1995–2003)		+
18. Med. hake – Merluccius gayi peruanus (30–49 cm)	Biomass (B)	VPA estimates (1995–2003) (Wosnitza-Mendo, personal communication)		+
	Fishing mortality (F)	VPA estimates (1995–2003)	+	
	Catches (C)	IMARPE catch statistics (1995–2003)		+
19. Large hake – Merluccius gayi peruanus (>50 cm)	Biomass (B)	VPA estimates (1995–2003) (Wosnitza-Mendo, personal communication)		+
	Fishing mortality (F)	VPA estimates (1995–2003)	+	
	Catches (C)	IMARPE catch statistics (1995–2003)		+
21. Small demersals	Catches (C)	IMARPE catch statistics (1995–1999)		+
22. Benthic elasmobranchs	Catches (C)	IMARPE catch statistics (1995–1999)		+
25. Medium demersal fish	Catches (C)	IMARPE catch statistics (1995–1999)		+
26. Medium sciaenids	Catches (C)	IMARPE catch statistics (1995–1999)		+
28. Catfish	Catches (C)	IMARPE catch statistics (1995–2002)		+
29. Chondrichthyans	Catches (C)	IMARPE catch statistics (1995–1999)		+
30. Seabirds	Biomass (B)	IMARPE survey (1995–2003) (Goya, personal communication)		+
31. Pinnipeds	Biomass (B)	IMARPE survey (1995–2003) (Goya, personal communication)		+

sources of bottom-up and top-down dynamics. Hake were also of special interest due to the drastic decreases in population size that followed the last strong EN (Guevara-Carrasco, 2004; Ballón et al., 2008). We specifically looked at mortality of the small size class to help interpret possible sources influencing the low recruitment.

3. Results

3.1. External drivers

The driver to phytoplankton biomass and composition improved the overall fit of the simulation, reducing *SS* by 2.7% (Fig. 2b) with greatest improvement during EN and the subsequent 3 year period (Fig. 2a). The driver to immigrant biomass (mesopelagics) reduced *SS* by 9.2% (Fig. 2b) with the greatest improvement in later years when biomasses were highest (Fig. 2a). *SS* for the EN year 1997–98 alone was not improved by the immigrant driver (Fig. 2a). Fishing rate changes proved to be the most important of the three external drivers overall, reducing *SS* by 22.0% (Fig. 2b). Improvements were observed throughout the simulated period except for the final year, and were generally more important during the post-EN years (Fig. 2a).

3.2. Best-fit vulnerabilities

The fit-to-time-series search for vulnerabilities revealed several important predator-prey interactions (Table 2), and further decreased *SS* by 31.2% after the application of the three internal drivers *PP*, *F*, and *I* (total decrease in *SS* of 64.3%). The results did not support a wasp-waist configuration for small pelagics (agrees with Ayón et al., 2008), as bottom-up configurations were estimated for sardines and anchovy on meso- and macrozooplankton; however, a bottom-up configuration was fit for interactions of sardine and anchovy, and their predators. Top-down control of macrozooplankton by mesopelagics and large hake was also suggested. The

Table 2
Predator–prey vulnerabilities searched in the fit-to-time-series routine (in bold); *BU* = bottom-up; *MX* = mixed/intermediate (default setting); *TD* = top-down.

Predator/prey	Diatoms	Silico- and Dinoflagellates	Microzooplankton	Mesozooplankton	Macrozooplankton	Sardine	Anchovy	Mesopelagics	Jumbo squid	Other small pelagics	Small hake	Small demersals	Conger	Med. sciaenids	P. stephanophrys
Mesozooplankton	**1 (BU)**	2 (MX)	2 (MX)												
Macrozooplankton	**1E+10 (TD)**	**1 (BU)**	**1E+10 (TD)**												
Sardine	2 (MX)	2 (MX)	2 (MX)	**1 (BU)**	**1 (BU)**										
Anchovy	**1E+10 (TD)**	2 (MX)	2 (MX)	**1 (BU)**	**1.16 (BU)**										
Mesopelagics				2 (MX)	**1E+10 (TD)**										
Jumbo squid				2 (MX)	2 (MX)		**1 (BU)**	**1 (BU)**	**1E+10 (TD)**	2 (MX)	**1E+10 (TD)**				
Other Cephalopods					**1 (BU)**							2 (MX)			
Horse mackerel					2 (MX)		**1 (BU)**			2 (MX)		2 (MX)			
Mackerel	2 (MX)		2 (MX)	2 (MX)	**1.55 (BU)**			2 (MX)				2 (MX)			
Other large pelagics							**1 (BU)**		2 (MX)	2 (MX)		2 (MX)			
Small hake					2 (MX)	**1 (BU)**	**1 (BU)**		**1 (BU)**	2 (MX)		2 (MX)			**1E+10 (TD)**
Med. Hake					2 (MX)		**1.16 (BU)**			**1E+10 (TD)**		**1E+10 (TD)**			**1.31 (BU)**
Large hake					**1E+10 (TD)**		**1 (BU)**	**1.02 (BU)**			**1E+10 (TD)**	**1.43 (BU)**	**1 (BU)**	**1E+10 (TD)**	**1E+10 (TD)**
Flatfish							**1 (BU)**								
Small demersals	**1E+10 (TD)**			**1E+10 (TD)**											
B. elasmobranchs					2 (MX)	**1 (BU)**	**1 (BU)**		2 (MX)	2 (MX)		2 (MX)	2 (MX)	2 (MX)	
Conger												2 (MX)			**1E+10 (TD)**
Med. demersal fish					2 (MX)		**1 (BU)**			2 (MX)		2 (MX)			
Med. sciaenids					2 (MX)	**1 (BU)**	**1 (BU)**	2 (MX)	2 (MX)	2 (MX)		2 (MX)		2 (MX)	
P. stephanophrys					**1 (BU)**										
Catfish				2 (MX)	2 (MX)		**1 (BU)**			2 (MX)					
Chondrichthyans							**1 (BU)**		2 (MX)		2 (MX)				
Seabirds							**1 (BU)**			2 (MX)		2 (MX)			
Pinnipeds							**1 (BU)**	2 (MX)		2 (MX)	2 (MX)	2 (MX)		2 (MX)	
Cetaceans					2 (MX)		**1 (BU)**		2 (MX)						

control of mesopelagic fish to its main predator, jumbo squid, was 1.0 (bottom-up), helping to explain the increase of squid biomass following the EN of 1997–98. The final time-series trends of the simulation versus the base data is shown in Fig. 3 for biomass and Fig. 4 for catch data.

3.3. Focus on main fishing targets

Anchovy changes during EN were best explained through bottom-up diatom and zooplankton availability, while later changes were more attributable to the fishery. Reduction in diatoms during EN resulted in a higher contribution of zooplankton in the anchovy diet. Dino- and silicoflagellate increases were unimportant as this group contributes only a small proportion to their diet generally (Fig. 5). During EN, modeled predation on anchovy increased – mainly due to horse mackerel – but non-predatory mortality was far stronger (Fig. 6) and seems due to low feeding rates and decreased prey availability. After EN, mortality rates were mainly controlled by fishing.

Decreases in the hake biomasses were well predicted by the simulation for all three size classes (Fig. 3). Mortalities for small juvenile hake indicate that cannibalism did not contribute greatly to the overall mortality even during the pre-crash years of 1995–96 and 1996–97 when adult biomass was higher. Modeled predation of small hake by jumbo squid remains fairly constant despite the squid increases. Squid predation does, however, represent a higher proportion of total hake mortality in the last simulation year following reduction of the hake fishery. Fishing is the most substantial source of mortality for all three hake groups, especially for medium and large hake (Fig. 7).

The immigrant driver simulated the immigration of mesopelagic fish into the model domain. One result is the increase in jumbo squid biomass and a shift in the jumbo squid's diet toward a larger proportion of mesopelagic fish (Fig. 8). Small hake, however, contributed minimally to the squid diet.

4. Discussion

We use the model for the 1995–96 year as a starting point for several reasons: (i) reliable, periodic sampling conducted by IMARPE began in 1995; (ii) 1995–96 was a fairly typical, "normal" upwelling year, several years after the recovery of anchovy; and (iii) 1995–96 preceded the strong EN of 1997–98, offering insight into subsequent dynamics. We asked the question whether this EN event has been a principal perturbation over 1995–2004 and to what degree trophic interactions played a role in the observed ecosystem changes.

4.1. Role of external drivers

Phytoplankton – Given the major decrease in primary production that occurs during EN, it was assumed that the application of this driver would have a major bottom-up impact through the trophic web, and would partially explain the decreased biomass of the coastal ecosystem as a whole. In fact, externally driving phytoplankton downwards did improve the fit of the simulation, especially during EN and the immediately following 3 years. Later years show a reduced importance of the forced phytoplankton changes, likely due to less yearly phytoplankton variability under the more "normal" upwelling conditions (Fig. 1b).

Copepods make up the majority of the mesozooplankton biomass in Peru and are known to be important grazers of the larger microphytoplankton (DeMott, 1989; Sommer et al., 2002, 2005). The model correctly predicts a decrease in mesozooplankton biomass in response to the decreased diatom biomass of 1997–98. Contrary to the sampled changes of mesozooplankton, a rapid recovery is predicted by the model following the resumed higher diatom and total phytoplankton biomass (Fig. 3). Without speculating too much as to the reasons for this discrepancy, we believe that much additional work is required in the modeling of zooplankton. Still, the model predicts at least the correct direction of change for many higher trophic groups, and in some cases predicts change of the correct magnitude as the base data. This is especially true of the trophically-important anchovy dynamics for which data is more widely available.

Of particular importance to small pelagic dynamics are particle size feeding preferences observed for the different species. Sardines possess fine-meshed gillrakers suitable for filtering smaller-sized particles. Anchovy, on the other hand, are more specialized and efficient at feeding on larger-sized particles (James and Findlay, 1989; van der Lingen, 1994; van der Lingen et al., 2006). The result of these adaptations, at least in the Benguelan populations, is that anchovy seem to have higher clearance rates (per weight) than sardine when available particles are larger than about 500–600 μm (van der Lingen, 1994). These feeding differences have been dealt with in other trophic models by defining separate zooplankton compartments by size, and through different vulnerabilities to grazing by small pelagics (Heymans and Baird, 2000; Shannon et al., 2003; Neira and Arancibia, 2004; Shannon et al., 2004a,b). We have further divided phytoplankton into two

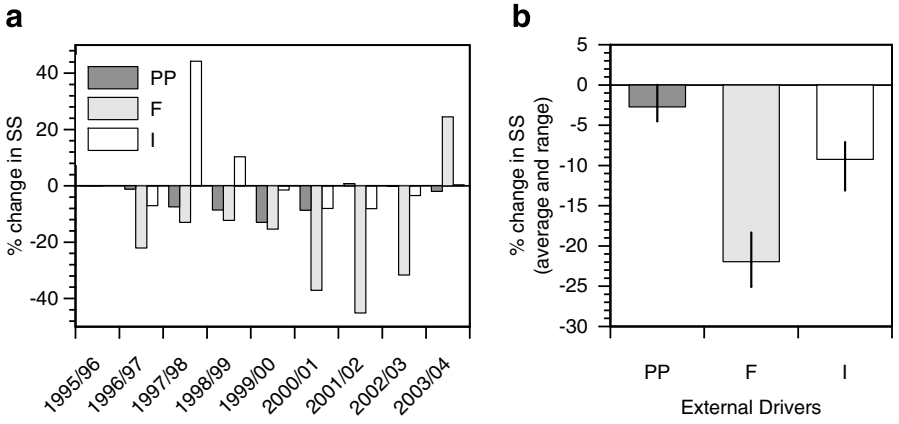

Fig. 2. Percent changes to sum of square differences, *SS*, after the application of different external 'drivers': phytoplankton biomass (*PP*); fishery rates (*F*); and immigrant biomass (*I*). (a) *SS* changes by year after the individual application of each external driver. (b) Average and range of *SS* changes under the application of external drivers in all possible sequences and combinations. All simulations use intermediate, default control settings (i.e. all predator–prey vulnerabilities equal 2.0). Negative values (i.e. decrease in *SS*) indicate an improvement in fit.

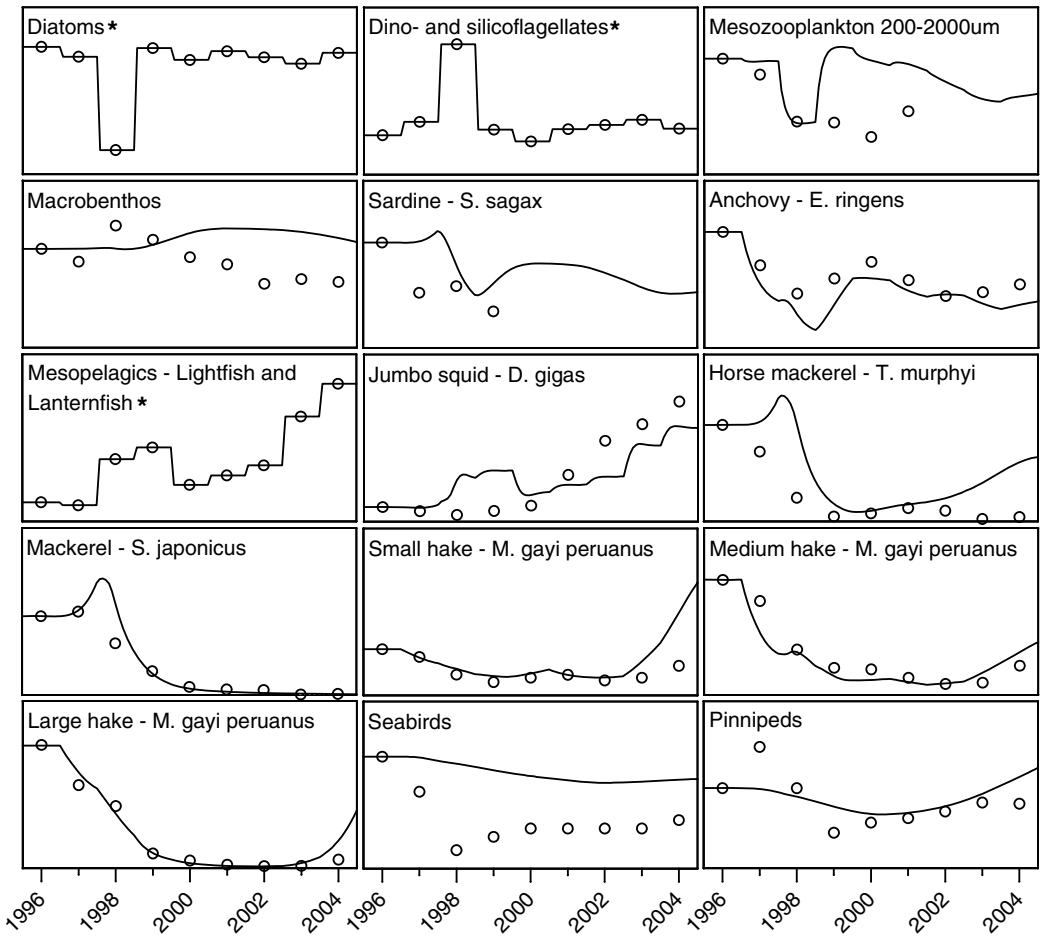

Fig. 3. Time-series trends of biomass changes from the data sets (dots) and Ecosim simulations (lines). Presented is the best-fit simulation (i.e. lowest *SS*), using all drivers (*PP*, *F*, and *I*) followed by a "fit-to-time-series" routine. Yearly data points represent "biological years" (i.e. July-June of following year). Asterisks (∗) indicate artificially-forced functional groups (diatoms, dino - and silicoflagellates, and mesopelagics).

taxonomic groups for a similar reason. According to the biovolume conversions of diet data conducted for our initial steady-state model (Tam et al., 2008) and other authors (Alamo, 1989; Espinoza and Blaskovic, 2000) anchovy feed more on diatoms than flagellates. Although diatoms are more associated with the nearshore cold habitat of the anchovy, they are usually smaller than the cited 500–600 μm optimal particle size; however, it seems likely that aggregates and cell-chains allow anchovies to filter even fairly small diatoms. As a result, anchovy dynamics are well simulated. The initial decrease in anchovy biomass during 1997–98 is mainly reproduced by forcing phytoplankton abundance downwards; specifically, a decrease in diatom biomass and, subsequently, a decrease in the second most important food item, mesozooplankton.

The modeled switch to an anchovy diet dominated by zooplankton was not as complete as was observed from *in situ* samples (Espinoza and Bertrand, 2008; Tam et al., 2008) (Fig. 5), possibly due to: (i) forced biomass decreases of phytoplankton may not have reduced diatoms as dramatically as in reality; (ii) anchovy move closer to the coast and deeper (up to 150 m) during EN (Bertrand et al., 2004), which may be due to non-trophic reasons (e.g. physiological stress associated with the higher surface water temperatures), and possibly prevent feeding upon the remaining diatom biomass; (iii) The modeled starting diet may have been too high (or not) in diatoms, although this cannot explain the lack of change in diet composition as this is calculated mainly from the changes in biomass and vulnerability. Espinoza and Bertrand (2008) have estimated the percent contribution of phytoplankton in carbon units to anchovy diet from stomach contents. Their results indicate that mesozooplankton and macrozooplankton comprise as much as 98% of carbon intake. Although their diet data still needs to be weighted according to the distribution of the anchovy population, it may indicate that our model overestimates the importance of phytoplankton as anchovy prey.

Fishing rates – The application of fishing as an external driver improved the fit of the simulation and helps to explain the long-term dynamics of several main target species. The fishing driver decreased long-term variance by 22%, as compared to a 2–3% decrease in a similar study for the Southern Benguela (Shannon et al., 2004a). This very large difference suggests strong fishery impact on the Peruvian system. In a comparison of trophic models, Moloney et al. (2005) illustrated that the South Benguelan fishery operates on a higher trophic level than in other EBCSs due to the differing diet of small pelagics and composition of the catch; specifically, Benguela small pelagics eat more zooplankton and fishery catches contain more demersal fish. The differences result in a higher mean trophic level of the catch in the Southern Benguela, elevating the statistic of *Flows required per unit of catch* ($[t\ 1^{\circ}\text{prod}]\ [t\ \text{catch}]^{-1}\ \text{km}^{-2}\ \text{y}^{-1}$) and indicating that the same tonnage catch requires more energetic input from the ecosystem. Despite this cost, the authors determined that the Southern Benguelan fishery required a smaller proportion of total primary production to sustain it when compared to the Peruvian fishery (4% vs. 10%), reflecting the much higher fishing rates in the Peruvian system.

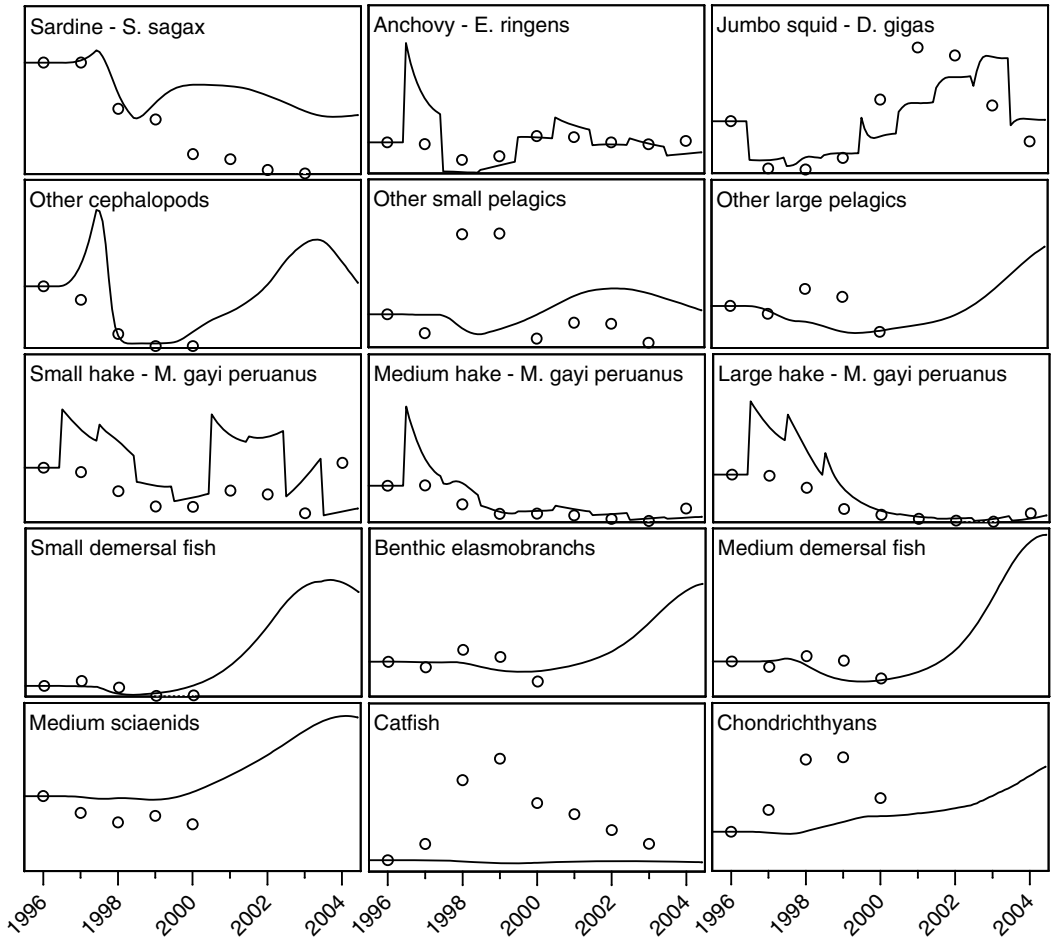

Fig. 4. Time-series trends of fisheries catch changes from the data sets (dots) and Ecosim simulations (lines). Presented is the best-fit simulation (i.e. lowest *SS*), using all drivers (*PP*, *F*, and *I*) followed by a "fit-to-time-series" routine for the 30 most sensitive predator-prey vulnerabilities. Yearly data points represent "biological years" (i.e. July–June of following year).

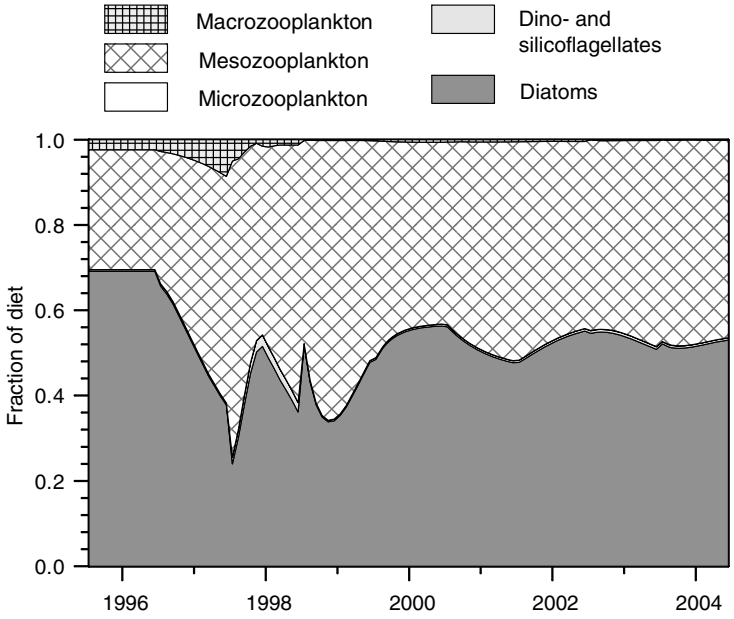

Fig. 5. Contribution of prey items to the diet of anchovy through the Ecosim simulation.

The simulation output calculates mortality rates through time, allowing for the determination of the importance of yearly fishing mortality changes for some key target groups' dynamics as discussed in the following sections. For anchovy, fishing mortality

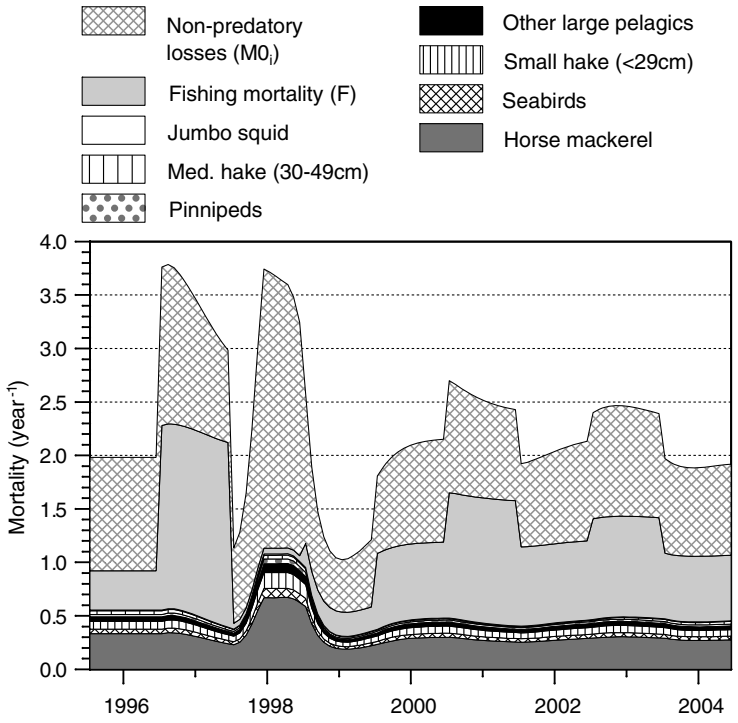

Fig. 6. Sources of mortality of anchovy, *Engraulis ringens*, through the Ecosim simulation. Only the top seven sources of predation mortality are shown (representing >95% of total predation mortality).

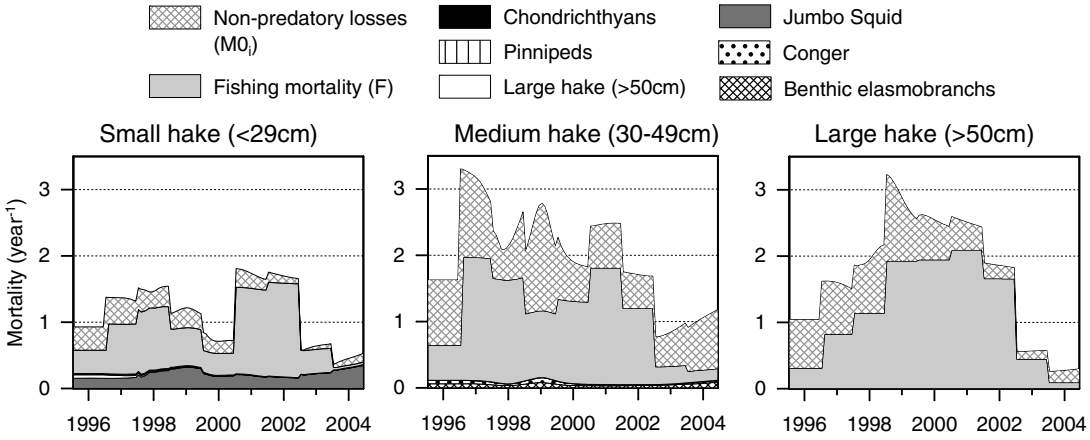

Fig. 7. Sources of mortality for different size classes of hake, *Merluccius gayi peruanus*, through the Ecosim simulation.

(*F*) values are much more variable than mortality from predation (Fig. 7). In 1996–97, before the onset of EN, VPA-derived *F* values more than doubled. This is consistent with past EN events whereby during the first phase of the EN stocks concentrate inshore, increasing their density and catchability (Csirke, 1989), whereas later, during the height of EN and possibly coinciding with the brunt of the arriving Kelvin wave, anchovy stocks are further driven inshore and/or to greater depths (Icochea, 1989; Bertrand et al., 2004). Anchovy had moved closer to the coast and to deeper waters (up to 150 m), which prevented large industrial purse seining (Arntz and Fahrbach, 1991; Bertrand et al., 2004). As the *F* values used are based on a biological year (July–June), the 1996–97 value is influenced by the onset of EN. Positive temperature anomalies for the Peruvian coast were noted as early as March 1997 and more than 2.8 million tonnes were landed during April and May alone. Shortly after these impressive catches, the anchovy fishery was essentially closed until the end of 1998, such that *F* was near zero during EN. Dynamics of the anchovy population in the later years of the simulation show both fishery and predation mortalities elevated as fishing began again and some predators recovered, causing some drop in anchovy biomass over 2000–2003 (Fig. 6).

According to the VPA analysis conducted by IMARPE, hake biomass was very high between 1993 and 96 – levels not seen since the late 1970s – however these levels declined dramatically after the EN of 1997–98 and have remained alarmingly low for the past decade. As a result, the hake fishery closed in September 2002 and now operates at a much smaller scale. Several hypotheses have been offered to explain the crash: (i) low recruitment-success due to cannibalism of juveniles by adult hake (Ballón, 2005), (ii) increased predation pressure on small hake due to the immigration/expansion of jumbo squid, (iii) overfishing (Wosnitza-Mendo et al., 2005), and (iv) demersal community changes affecting the prey of hake (Ballón, 2005). The simulated mortalities for small juvenile hake suggests that cannibalism does not contribute much to

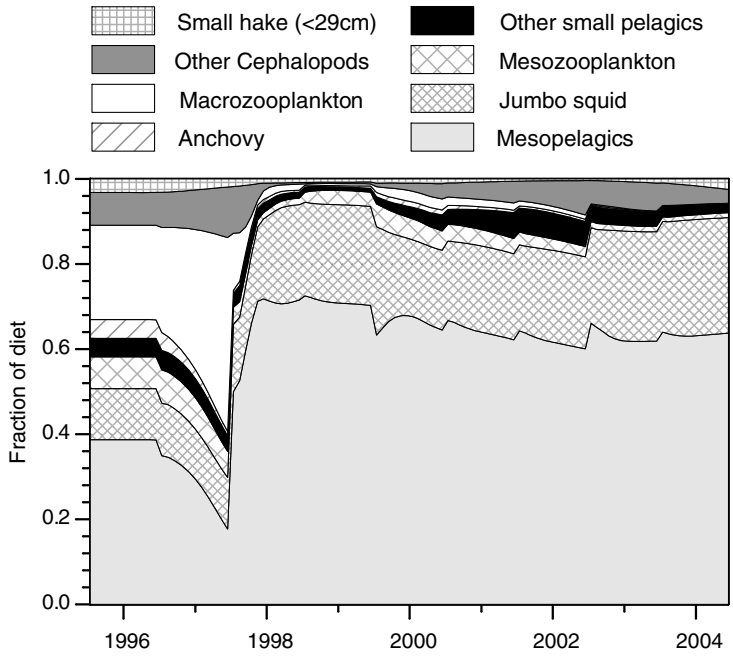

Fig. 8. Contribution of prey items to the diet of jumbo squid, *Dosidicus gigas*, through the Ecosim simulation.

mortality even when adult hake were abundant (1995–97; Fig. 7). Hake fishing mortality, however, increased before EN and remained at high levels for all three hake size groups until the fishery closure in 2002. These increases in F over the EN period, in contrast to previous ENs during which F generally decreases, were likely due to improved fishing techniques and movement of the trawl fleet southwards in pursuit of hake (Wosnitza-Mendo et al., 2005). The model suggests further mortality occurred due to decreases in prey abundance, especially for medium and large hake. This result is supported by Ballón et al. (2008), who found for 1972–2004 that gonadosomatic and stomach fullness indices decreased with EN-associated positive temperature anomalies, implying food-limited somatic production. The simulation predicts biomass gains for all three hake groups during 2003–04 due to reduced fishing mortality after 2001; however, hake did not recover in reality (Fig. 3). Ballón et al. (2008) offer a non-trophic explanation – reproductive failure. They observed that while large hake (>35 cm) show high condition and stomach fullness indices during the 2000s, gonadosomatic indices have decreased since the mid 1980s. Additionally, sex ratios have shifted toward females (reaching almost 100% for fish larger than 35 cm), leading the authors to hypothesize that long-term fishing pressure from the fishery may have disproportionately depleted males (males comprised 80% of the catches during the 1980s) to the point where females now lack a sufficient number of males to stimulate reproduction. Such a dependence on males to induce spawning is typical in cod-like species (Rowe and Hutchings, 2003). Nevertheless, our simulation supports the results of the VPA: Increases in F explain the sharp decline in hake abundance observed from 1997 to 2002. When compared to the baseline natural mortality value ($M = 0.38$) used in the VPA, total mortality values (Z) sum to extremely high levels (above 2.0) for medium and large hake groups, mainly driven by F, and illustrate the pressure put on the group during the post-EN period.

Time-series data on fishing rates existed for only three species at the time of this study (anchovy, hake, and jumbo squid). Therefore, simulation results concerning the importance of the fisheries on system dynamics may be somewhat conservative and future simulations may observe an even greater importance by incorporating additional fisheries.

Immigration – The offshore border of the model domain was set at 60 nm (ca. 111 km), which is approximately the mean width of the continental shelf. Previous model domains for the Peruvian upwelling system (Jarre et al., 1991) were narrower due to focus on the nearshore habitat of anchovy. Our wider domain allowed incorporation of the "active zone" or productive upwelling system (Nixon and Thomas, 2001). Our latitudinal range (4–16°S) similarly encompassed the main upwelling region delimited by the equatorial current to the north and a zone of decreased offshore Ekman transport further to the south. This latitudinal extension also corresponds to the main distribution of the northern Humboldt sardine and anchovy stocks (Alheit and Ñiquen, 2004). Despite this care to account for variability of principal functional groups, several less coastal species migrate into the model area, especially during periods of reduced upwelling and subsequent habitat reduction associated with EN. Sardine and mackerels, for example, remain offshore in oceanic water during the strong upwelling of La Niña (Bertrand et al., 2004); and it has been hypothesized that physiological restraints may also limit their distribution (Jarre et al., 1991). These non-trophic effects may help to explain why some more oceanic groups' dynamics are not well predicted by the model, and thus may require additional external forcing in future simulations.

The immigration of mesopelagic fish during EN does not appear to have been a significant factor for the decreased biomass of more coastal species during the EN 1997–98. However, their longer-term growth does appear to impact some more coastal groups in later years of the simulation when their mesopelagic biomass was highest. While the cause of the mesopelagic fish outburst is not known, we speculate that either (i) the euphausiids biomass increased during EN in response to decreased grazing competition with mesozooplankton, and/or (ii) the deepened thermocline during EN may have increased the vulnerability of euphausiids – a principal prey for mesopelagic fish – allowing for an increase in predation by mesopelagic fish. Given euphausiids' strategy of predation avoidance through diel vertical migrations across the Oxygen Minimum Layer (OML, <1.0 ml L^{-1}) (Antezana, 2002), it is possible that a deepening of the upper boundary of the OML may have caused increased vulnerability to predation. In any case, this increase in mesopelagic fish biomass during and after the EN helps to explain

the decreases in biomass of both mackerel groups through competition for macrozooplankton, a main prey for all three.

Another link with the mesopelagic fish expansion is the bottom-up response of the key predator, jumbo squid. This has had some benefits in Peru through the sale of fishing permits to foreign offshore Japanese and Korean jigging vessels as well as becoming an important target species for the nearshore artisanal fisheries. Despite this, the fear of negative effects of the jumbo squid outburst on the more valuable hake population has caused alarm. The results of this study indicate that while some competitive effects do occur between jumbo squid and hake, the high fishing rates appear to have more responsibility in the hake's decline. While the direct predation mortality rates on small hake by jumbo squid appear relatively stable in the simulation, is should be noted that it is proportionally larger in the later years possibly due to groups' lower total mortality (Fig. 7).

4.2. Internal control mechanisms

The dramatic improvement in *SS* (31.2%) after the fit-to time-series routine highlights the importance of trophic control to internal dynamics of the ecosystem. Shannon et al. (2004a) also found that fitting of internal dynamics improved the simulation in the Southern Benguela by 40%. Our shorter time-series makes for a less robust analysis; however, we will focus on the most important and interpretable interactions.

One of the more significant results of the vulnerability fitting exploration was that a wasp-waist configuration around small pelagics, typical for other EBCSs, is not supported for the Peruvian system. Cury et al. (2000) found a negative relationship between yearly zooplankton concentrations and small pelagic landings for several upwelling systems (California, Ghana and Ivory Coast, Oyashio (Japan), Black Sea, Southern Benguela) and hypothesized that zooplankton biomass is top-down controlled by pelagic fish. Shannon et al., (2004a), Shannon et al., (2004b) further supported a wasp-waist configuration surrounding small pelagics in the Southern Benguela system. On the other hand, Cury et al. (2000) mentioned that the Peruvian system was one of the few exceptions where zooplankton concentrations and small pelagic landings were positively correlated; specifically, lower zooplankton concentrations (mainly mesozooplankton is sampled) were observed off Peru during the mid 1970s to mid 1980s, coinciding with the period after the anchovy collapse. Zooplankton concentrations have since increased with the recovery of anchovy, but remain lower than the concentrations of the 1960s and early 1970s (Ayón et al., 2004). For the shorter time-series modeled here, we also found a bottom-up relationship between mesozooplankton and the predators – anchovy and sardine (agrees with Ayón et al. 2008).

It has been proposed that Peru's proximity to the equator allows for optimal conditions for upwelling and fish production (Cury and Roy, 1989; Bakun, 1996), by allowing plankton communities to become particularly rich above the stable and relatively shallow thermocline. Furthermore, the shallow oxygen minimum may concentrate plankton above it, thus improving the grazing efficiency of small pelagic fish. We have demonstrated the importance of diatoms in the dynamics the Humboldt Current System, yet to the best of our knowledge a comparison of phytoplankton composition (i.e. based on cell size, taxa, unicellular vs. chain-forming, etc.) between EBCSs is lacking, thus preventing speculation if differences in phytoplankton composition exist. Highly concentrated plankton in Peru would not necessarily explain why zooplankton and small pelagics would both benefit simultaneously during periods of high upwelling. In fact, highly concentrated plankton might make top-down grazing pressure even more pronounced due to more efficient filter-feeding by anchovy. This possibility is supported by Ayón et al. (2008) through evidence of top-down control on smaller scales in Peru, wherein zooplankton biovolume is lower where anchovy and sardine biomass is high (acoustically determined, within a 5 km radius of the zooplankton sample). This finding is contrary to the negative correlation between large-scale trends of zooplankton volumes versus small pelagic fish biomass (Cury et al., 2000); however, Ayón et al. mention the importance of scale in explaining this discrepancy.

Cury et al. (2000) found negative relationships between zooplankton and small pelagics abundances in several upwelling systems (Ghana and Ivory Coast; Southern Benguela; Oyashio, Japan), yet the finding may be in part due to sampling bias, as zooplankton time-series tend to be based on samples restricted to the continental shelf. Where zooplankton over a larger extension from the coast and with evenly spaced sampling stations (California), no significant correlation to small pelagic catches is found. Similarly, zooplankton sampling conducted by IMARPE is fairly uniform and extends to ca. 185 km (100 nm) from the coast. This does not eliminate the possibility of wasp-waist forcing in Peru, but it does imply that it may occur only on smaller scales than our model domain.

Bottom-up configurations were found between sardine and anchovy to all their higher predator groups. In particular, the decreases in anchovy biomass associated with EN contributed to the decreases in several predatory groups, especially horse mackerel and small hake. Over longer time scales (i.e. decadal), both of these fish species show flexibility in their diets, especially during periods of low anchovy biomass (mid 1970s to late 1980s) – horse mackerel shift to zooplankton (Muck, 1989) and hake shift to sardine (Castillo et al., 1989). The shorter simulation period of this study appears to capture the reduction in system size due to the reduced upwelling during EN. As a result, most functional groups of the coastal environment experience reductions in biomass, which may differ from dynamics on decadal time scales such as a regime change. Generally, our results support previous studies presented in Pauly and Tsukayama (1987a), where teleosts, especially horse mackerel, are far more important consumers of anchovy than guano birds and pinnipeds; however acoustic surveys show that teleost spatial overlap with anchovy appears to have decreased significantly since 1997 (A. Bertrand, personal communication).

A more probable bottom-up relationship is that between anchovy and seabirds and pinnipeds, whose distributions strongly overlap with anchovy habitat. Even with a forced bottom-up configuration to anchovy, the model did not reproduce the large decreases in seabirds and pinnipeds that were observed following EN. We believe that a reduction in anchovy vulnerability may explain such a result. Muck and Pauly (1987) first proposed that seabirds are probably more affected by changes in vulnerability resulting from sea surface temperature-mediated distribution changes of anchovy than by changes in anchovy biomass. As mentioned earlier, not only did anchovy retreat to remaining centers of upwelling during EN (Alheit and Ñiquen, 2004), but also moved deeper (up to 150 m) with the thermocline (Bertrand et al., 2004). We believe that this movement made them less vulnerable to these predators. This is well illustrated in a diagram presented by Jarre et al. (1991) whereby changes in the vertical distribution of anchovy affect their vulnerability to predation or capture from seabirds, pinnipeds, and purse seiners. Diving seabirds are specialists on anchovy and have the shallowest effective hunting depth, and so would become the most susceptible to changes in the anchovy's vertical distribution.

Other important internal controls are observed with the more oceanic-associated functional groups. The expansion / immigration of mesopelagic fish into the model area impacted several groups directly, including possible top-down forcing of macrozooplankton and bottom-up forcing to jumbo squid. As mentioned before, this

result must be taken with caution given that the diet of mesopelagic fish was not based on *in situ* measurements during the model period; however, the inclusion of several interactions involving macrozooplankton as prey in the vulnerability fitting routine suggests that their dynamics may be of more importance than previously thought. In particular, a top-down configuration between mesopelagics and macrozooplankton helped to explain decreases in macrozooplankton biomass, and subsequent decreases in several competitors for macrozooplankton (other cephalopods, mackerel, horse mackerel). While these groups' are more oceanic, they nevertheless have connections to the coastal zone. Mackerels are known to come closer to the coast both seasonally and during EN in response to decreased upwelling, where they may impact anchovy and other coastal species. Jumbo squid and other cephalopods also occur across the shelf. Cephalopods populations are subject to dramatic fluctuations and their impact on prey populations is equally variable. Their role as predators on fish and crustaceans clearly implicates them as a factor influencing natural mortality and recruitment-success in stocks of commercial exploited species (Rodhouse and Nigmatullin, 1996).

4.3. Conclusions and future prospects

The introduction of external drivers has allowed us to reproduce several key dynamics of the Northern Humboldt Current Ecosystem. Changes in phytoplankton associated with ENSO are important on the short-term while fishing rates and immigration from outside the upwelling region are important dynamics in the long-term. This has helped to elucidate that the dynamics of the Humboldt Current Ecosystem associated with the impact of an El Niño event appear to be relatively restricted to the immediate years following the event, and that once normalization returns, the management of fishing rates will be increasingly important. The separation of principal phytoplankton taxa allows for the simulation of important changes of energy flow in the Northern Humboldt Current Ecosystem over several temporal scales. Additionally, a link between the dynamics of the phytoplankton components and more easily observable environmental parameters, i.e. SST anomalies, takes a first step in the development of predictive models forced in real time.

A larger offshore extension allowed for the incorporation of important interactions between the coastal and more oceanic components of the ecosystem. Nevertheless, artificial forcing of mesopelagic fish was still necessary in reproducing the dynamics of the more oceanic-associated groups. Further investigation into the underlying drivers of the offshore ecosystem may become increasingly important in describing the dynamics of the more economically-important coastal upwelling system.

Internal control settings showed a mix of interactions; however a "wasp-waist" configuration around small pelagic fish is not supported. Specifically, top-down forcing of meso- and macrozooplankton by small pelagic fish is not observed.

Additional non-trophic interactions may also play important roles in dynamics (e.g. changes in vulnerability, recruitment, physiological constraints), and must be considered in future modeling efforts. We have highlighted possibilities of these in cases where the model fails to reproduce the historical trends. This has been an unexpected but extremely positive outcome of the two parts of this work, and has helped to formulate further questions and investigation foci for the future.

Finally, future prospects for trophic modeling include the adaptation of longer reconstructed time-series by Pauly and Tsukayama (1987b), Pauly et al. (1989) and Guenette et al. (this issue) to the model in order to explore dynamics since the development of the industrial fishery around the 1950s. This would create a more robust analysis by which to further tune the internal forcing controls of the model, including the larger-scale dynamics of a regime shift. Ultimately, this will allow for further exploration of fishing scenarios for improved management of the ecosystem.

Acknowledgements

The authors acknowledge assistance from the following people (in alphabetical): Milena Arias-Schreiber, Arnaud Bertrand, David Correa, Michelle Graco, Renato Guevara, Mariano Gutierrez, Kristen Kaschner, Miguel Ñiquen, Ralf Schwamborn, Sonia Sánchez, and Carmen Yamashiro. We also thank Carl Walters for the use of the Ecosim software, and Dr. Lynne Shannon and an anonymous referee for their critical suggestions on the manuscript. This study was financed and conducted in the frame of the EU-project CENSOR (Climate variability and El Niño Southern Oscillation: Impacts for natural resources and management, contract No. 511071) and is CENSOR publication No. 0086.

References

Alamo, A., 1989. Stomach contents of anchoveta (*Engraulis ringens*), 1974–1982. In: Pauly, D., Muck, P., Mendo, J., Tsukayama, I. (Eds.), The Peruvian Upwelling Ecosystem: Dynamics and Interactions, 391. ICLARM, Manila, Philippines, pp. 105–108.

Alheit, J., Ñiquen, M., 2004. Regime shifts in the Humboldt Current ecosystem. Progress in Oceanography 60, 201–222.

Antezana, T., 2002. Adaptive behavior of *Euphausia mucronata* in relation to the oxygen minimum layer of the Humboldt Current. In: Färber Lorda, J. (Ed.), Oceanography of the Eastern Pacific. CICESE, Ensenada, Mexico, pp. 29–40.

Arntz, W.E., Fahrbach, E., 1991. El Nino-Klimaexperiment der Natur. Birkhauser Verlag, Basel, Switzerland.

Avaria, S., Muñoz, P., 1987. Effects of the 1982–1983 El Niño on the marine phytoplankton off northern Chile. Journal of Geophysical Research 92, 14369–14382.

Ayón, P., Purca, S., Guevara-Carrasco, R., 2004. Zooplankton volume trends off Peru between 1964 and 2001. ICES Journal of Marine Science 61, 478–484.

Ayón, P., Swartzman, G., Bertrand, A., Gutierrez, M., Bertrand, S., 2008. Zooplankton and forage fish species off Peru: large-scale bottom-up forcing and local-scale depletion. Progress in Oceanography. 79, 208–214.

Baird, D., McGlade, J.M., Ulanowicz, R.E., 1991. The comparative ecology of six marine ecosystems. Philosophical Transactions: Biological Sciences 333, 15–29.

Bakun, A., 1996. Patterns in the ocean. Ocean processes and marine population dynamics. University of California Sea Grant, California, USA, in cooperation with Centro de Investigaciones Biologicas de Noroeste, La Paz, Baja California Sur, Mexico.

Bakun, A., Weeks, S.J., 2008. The marine ecosystem off Peru: What are the secrets of its fishery productivity and what might its future hold? Progress in Oceanography. 79, 290–299.

Ballón, M., Wosnitza-Mendo, C., Guevara-Carrasco, R., Bertrand, A., 2008. The impact of overfishing and El Niño on the condition factor and reproductive success of Peruvian hake, *Merluccius gayi peruanus*. Progress in Oceanography 79, 300–307.

Ballón, R.M., 2005. Comparative analysis of the community structure and trophic relations of the Peruvian hake *Merluccius gayi peruanus* and its by-catch of the years 1985 and 2001. Masters Thesis, University of Bremen, Bremen, Germany, unpublished.

Bertrand, A., Segura, M., Gutierrez, M., Vasquez, L., 2004. From small-scale habitat loopholes to decadal cycles: a habitat-based hypothesis explaining fluctuation in pelagic fish populations off Peru. Fish and Fisheries 5, 296–316.

Bidigare, R.R., Ondrusek, M.E., 1996. Spatial and temporal variability of phytoplankton pigment distributions in the Central Equatorial Pacific Ocean. Deep-Sea Research II 43, 809–833.

Brown, P.C., Painting, S.J., Cochrane, K.L., 1991. Estimates of phytoplankton and bacterial biomass production in the northern and southern Benguela ecosystems. South African Journal of Marine Science 11, 537–564.

Brush, M.J., Brawley, J.W., Nixon, S.W., Kremer, J.N., 2002. Modeling phytoplankton production: Problems with the Eppley curve and an empirical alternative. Marine Ecology Progress Series 238, 31–45.

Carr, M.E., 2002. Estimation of potential productivity in eastern boundary currents using remote sensing. Deep-Sea Research II 49, 59–80.

Castillo, R., Juárez, L., Higginson, L., 1989. Predación y canibalísmo en la población de la merluza peruana en el área de Paita-Peru. Memorias del Simposio Internacional de los Recursos Vivos y las Pesquerías en el Pacífico Sudeste, Viña del Mar, Chile, Revista Pacífico Sur (Número Especial).

Chavez, F.P., Ryan, J., Lluch-Cota, S.E., Ñiquen, M., 2003. From anchovies to sardines and back: multidecadal change in the Pacific Ocean. Science 299, 217–221.

Csirke, J., 1989. Changes in the catchability coefficient in the Peruvian anchoveta (*Engraulis ringens*) fishery. In: Pauly, D., Muck, P., Mendo, J.,Tsukayama, I. (Eds.), The Peruvian Upwelling Ecosystem: Dynamics and Interactions, vol. 18. ICLARM Conference Proceedings, Manila, Philippines, pp. 207–219.

Cury, P., Roy, C., 1989. Optimal environmental window and pelagic fish recruitment success in upwelling areas. Canadian Journal of Fisheries and Aquatic Sciences 46, 670–680.

Cury, P., Bakun, A., Crawford, R.J., Jarre, A., Quinones, R.A., Shannon, L.J., Verheye, H.M., 2000. Small pelagics in upwelling systems: patterns of interaction and structural changes in "wasp-waist" ecosystems. ICES Journal of Marine Science 57, 603–618.

DeMott, W.R., 1989. Optimal foraging theory as a predictor of chemically mediated food selection by selection by suspension-feeding copepods. Limnology and Oceanography 34, 140–154.

Espinoza, P., Blaskovic, V., 2000. Changes in diet of Peruvian anchoveta *Engraulis ringens* and its influence on feeding dynamics. Boletin del Instituto del Mar del Peru 19, 21–27.

Espinoza, P., Bertrand, A., 2008. Revising Peruvian anchovy (*Engraulis ringens*) trophic niche and ecological role reveals its plasticity and provides a new vision of the Humboldt Current system. Progress in Oceanography. 79, 215–227.

González, H., Daneri, G., Figueroa, D., Iriarte, J., Lefevre, G., Pizarro, G., Nones, R.Q., Sobrazo, M., Troncoso, A., 1998. Producción primaria y su destino en la trama trófica-pelágica y océano profundo e intercambio océano-atmósfera de CO_2 en la zona norte de la Corriente de Humboldt (23 S): Posibles efectos del evento El Niño, 1997– 1998 en Chile. Revista Chilena de Historia Natural 71, 429–458.

González, H.E., Giesecke, R., Vargas, C.A., Pavez, A., Iriarte, J., Santibáñez, P., Castro, L., Escribano, R., Pagès, F., 2004. Carbon cycling through the pelagic foodweb in the northern Humboldt Current off Chile (23° S). ICES Journal of Marine Science 61, 572–584.

Guevara-Carrasco, R., 2004. Peruvian hake overfishing: misunderstood lessons. Boletín del Instituto del Mar del Perú 21, 27–32.

Heymans, J.J., Baird, D., 2000. A carbon flow model and network analysis of the northern Benguela upwelling system, Namibia. Ecological Modelling 126, 9–32.

Heymans, J.J., Shannon, L.J., Jarre, A., 2004. Changes in the northern Benguela ecosystem over three decades: 1970s, 1980s, and 1990s. Ecological Modelling 172, 175–195.

Icochea, L., 1989. Análisis de la pesquería de arrastre pelágica en la costa peruana durante el período 1983–1987 y su relación con los cambios oceanográficos. Flota Pesquera Peruana (FLOPESCA), 51 S.

Iriarte, J.L., González, H.E., 2004. Phytoplankton size structure during and after the 1997/98 El Nino in a coastal upwelling area of the northern Humboldt Current System. Marine Ecology Progress Series 269, 83–90.

James, A.G., Findlay, K.P., 1989. Effect of particle size and concentration on feeding behaviour, selectivity and rates of food ingestion by the Cape Anchovy *Engraulis capensis*. Marine Ecology Progress Series 50, 275–294.

Jarre-Teichmann, A., 1992. Steady-state modelling of the Peruvian upwelling ecosystem. Ph.D. Thesis, University of Bremen, Bremen, Germany, unpublished.

Jarre, A., Muck, P., Pauly, D., 1991. Two approaches for modelling fish stock interactions in the Peruvian upwelling ecosystem. ICES Marine Science Symposia 193, 178–184.

Landry, M.R., Kirshtein, J., Constantinou, J., 1996. Abundances and distributions of picoplankton populations in the Central Equatorial Pacific from 12° N to 12° S, 140° W. Deep-Sea Research II 43, 871–890.

Moloney, C.L., Jarre, A., Arancibia, H., Bozec, Y.-M., Neira, S., Jean-Paul Roux, J.-P., Shannon, L.J., 2005. Comparing the Benguela and Humboldt marine upwelling ecosystems with indicators derived from inter-calibrated models. ICES Journal of Marine Science 62, 493–502.

Muck, P., Pauly, D., 1987. Monthly anchoveta consumption of guano birds, 1953 to 1982. In: Pauly, D., Tsukayama, I. (Eds.), The Peruvian Anchoveta and its Upwelling Ecosystem: Three Decades of Change, vol. 391. ICLARM, Manila, Philippines, pp. 219–233.

Muck, P., 1989. Major trends in the pelagic ecosystem off Peru and their implications for management. In: Pauly, D., Muck, P., Mendo, J., Tsukayama, T. (Eds.), The Peruvian Upwelling Ecosystem: Dynamics and Interactions, vol. 18. ICLARM Conference Proceedings, Manila, Philippines, pp. 386–403.

Neira, S., Arancibia, H., 2004. Trophic interactions and community structure in the upwelling system off Central Chile (33–39° S). Journal of Experimental Marine Biology and Ecology 312, 349–366.

Neira, S., Arancibia, H., Cubillos, L., 2004. Comparative analysis of trophic structure of commercial fishery species off Central Chile in 1992 and 1998. Ecological Modelling 172, 233–248.

Nixon, S., Thomas, A., 2001. On the size of the Peru upwelling ecosystem. Deep-Sea Research I 48, 2521–2528.

Ochoa, N., Rojas de Mendiola, B., Gómez, O., 1985. Identificación del fenómeno El Niño a través de los organismos fitoplanctónicos. Boletin del Instituto del Mar del Perú, Volumen extraordinario. Instituto del Mar del Perú, Callao, Peru. pp. 23–31.

Pauly, D., Tsukayama, I., 1987a. On the implementation of management-oriented fishery research: The case of Peruvian anchoveta. In: Pauly, D., Tsukayama, I. (Eds.), The Peruvian Anchoveta and Its Upweling Ecosystem: Three Decades of Change, vol. 391. ICLARM, Manila, Philippines, pp. 1–13.

Pauly, D., Tsukayama, I., 1987b. The Peruvian anchoveta and its upwelling ecosystem: three decades of change. ICLARM, Manila, Philippines.

Pauly, D., Muck, P., Mendo, J., Tsukayama, I., 1989. The Peruvian upwelling ecosystem: Dynamics and interactions. In: ICLARM Conference Proceedings, Manila, Philippines.

Pennington, J.T., Mahoney, K.L., Kuwahara, V.S., Kolber, D.D., Calienes, R., Chavez, F.P., 2006. Primary production in the eastern tropical Pacific: A review. Progress in Oceanography 69, 285–317.

Pitcher, G.C., Brown, P.C., Mitchell-Innes, B.A. 1992. Spatio-temporal variability of phytoplankton in the southern Benguela Upwelling system. South African Journal of Marine Science/Suid-Afrikaanse Tydskrif vir Seewetenskap.

Purca, S., 2005. Variabilidad temporal de baja frecuencia en el Ecosistema de la Corriente de Humboldt frente a Perú. Ph.D. thesis, Universidad de Concepción, Concepción, Chile, unpublished.

Rodhouse, P.G., Nigmatullin, C.M., 1996. The role of cephalopods in the world's oceans. Role as consumers. Philosophical Transactions: Biological Sciences 351, 1003–1022.

Rojas de Mendiola, S., 1981. Seasonal phytoplankton distribution along the Peruvian coast. In: Richards, F.A. (Ed.), Coastal Upwelling, vol. 20. American Geophysical Union, Washington, DC, pp. 348–356.

Rowe, S., Hutchings, J.A., 2003. Mating systems and the conservation of commercially exploited marine fish. Trends in Ecology and Evolution 18, 567–572.

Sea Around Us, 2006. A global database on marine fisheries and ecosystems. Fisheries Centre, University British Columbia, Vancouver, Available from: <www.seaaroundus.org>.

Shannon, L.J., Moloney, C.L., Jarre, A., Field, J.G., 2003. Trophic flows in the southern Benguela during the 1980s and 1990s. Journal of Marine Systems 39, 83–116.

Shannon, L.J., Christensen, V., Walters, C.J., 2004a. Modelling Stock Dynamics in the Southern Benguela Ecosystem for the Period 1978–2002. African Journal of Marine Science 26, 179–196.

Shannon, L.J., Field, J.G., Moloney, C.L., 2004b. Simulating anchovy-sardine regime shifts in the southern Benguela ecosystem. Ecological Modelling 172, 269–281.

Sommer, U., Stibor, H., Katechakis, A., Sommer, F., Hansen, T., 2002. Pelagic food web configurations at different levels of nutrient richness and their implications for the ratio fish production: primary production. Hydrobiologia 484, 11–20.

Sommer, U., Hansen, T., Blum, O., Holzner, N., Vadstein, O., Stibor, H., 2005. Copepod and microzooplankton grazing in mesocosms fertilised with different Si:N ratios: no overlap between food spectra and Si:N influence on zooplankton trophic level. Oecologia 142, 274–283.

Sun, J., Liu, D., 2003. Geometric models for calculating cell biovolume and surface area for phytoplankton. Journal of Plankton Research 25, 1331–1346.

Tam, J., Taylor, M.H., Blaskovic, V., Espinoza, P., Ballón, R.M., Díaz, E., Wosnitza-Mendo, C., Argüelles, J., Purca, S., Ayón, P., Quipuzcoa, L., Gutiérrez, D., Goya, E., Ochoa, N., Wolff, M., 2008. Trophic flows in the Northern Humboldt Current Ecosystem, Part 1: Comparing 1995–96 and 1997–98. Progress in Oceanography.

Taylor, M.H., Wolff, M., 2007. Trophic modeling of Eastern Boundary Current systems: a review and prospectus for solving the "Peruvian Puzzle". Revista Peruana de Biologia 14, 87–100.

van der Lingen, C.D., 1994. Effect of particle size and concentration on the feeding behaviour of adult pilchard *Sardinops sagax*. Marine Ecology Progress Series 109, 1–13.

van der Lingen, C.D., Hutchings, L., Field, J.G., 2006. Comparative trophodynamics of anchovy *Engraulis encrasicolus* and sardine *Sardinops sagax* in the southern Benguela: are species alternations between small pelagic fish trophodynamically mediated? African Journal of Marine Science 28, 465–477.

Walsh, J.J., 1981. A carbon budget for overfishing off Peru. Nature 290, 300–304.

Walters, C., Christensen, V., Pauly, D., 1997. Structuring dynamic models of exploited ecosystems from trophic mass-balance assessments. Reviews in Fish Biology and Fisheries 7, 139–172.

Walters, C., Pauly, D., Christensen, V., Kitchell, J.F., 2000. Representing density dependent consequences of life history strategies in aquatic ecosystems: EcoSim II. Ecosystems 3, 70–83.

Walters, C.J., Martell, S.J.D., 2004. Fisheries Ecology and Management. Princeton University Press, Princeton, New Jersey.

Wosnitza-Mendo, C., Mendo, J., Guevara-Carrasco, R., 2005. Políticas de gestión para la reducción de la capacidad excesiva de esfuerzo pesquero en Perú: el caso de la pesquería de la merluza. In: Agüero, M. (Ed.) Capacidad de pesca y manejo pesquero en América Latina y el Caribe, vol. 461. FAO Technical Papers, pp. 343–372.